Published in final edited form as:
Am J Med Genet A. 2011 June ; 0(6): 1314–1321. doi:10.1002/ajmg.a.33980.

Genomic Strategy Identifies a Missense Mutation in *WD-Repeat Domain 65* (*WDR65*) in an Individual with Van der Woude Syndrome

Nicholas K. Rorick[1,2], **Akira Kinoshita**[1], **Jason Weirather**[2], **Myriam Peyrard-Janvid**[3], **Renata L. L. Ferreira de Lima**[4], **Martine Dunnwald**[1,2], **Alan L. Shanske**[5], **Danilo Moretti-Ferreira**[6], **Hannele Koillinen**[7], **Juha Kere**[3,8,9], **Maria A. Mansilla**[1], **Jeffrey C. Murray**[1,2], **Steve L. Goudy**[10], and **Brian C. Schutte**[11]

[1]Department of Pediatrics, University of Iowa, Iowa City, IA, USA [2]Interdisciplinary Graduate Program in Genetics, University of Iowa, Iowa City, IA, USA [3]Department of BioNut, Novum, Karolinska Institutet, Huddinge, Sweden [4]General Biology, Federal University of Bahia, Salvador, Bahia, Brazil [5]Center for Craniofacial Disorders, Children's Hospital at Montefiore, Bronx, NY, USA [6]Servico de Aconselhamento Genetico, Universidade Estadual Paulista, Botucatu, SP, Brazil [7]Department of Pediatrics, Turku University Hospital, Turku, Finland [8]Mutation Analysis Core Facility, Clinical Research Centre, Karolinska Institutet, Huddinge, Sweden [9]Department of Medical Genetics, University of Helsinki, Helsinki, Finland [10]Department of Otolaryngology, Vanderbilt University, Nashville, TN, USA [11]Departments of Microbiology and Molecular Genetics and Pediatrics and Human Development, Michigan State University, East Lansing, MI, USA

Abstract

Genetic variation in the transcription factor Interferon Regulatory Factor 6 (*IRF6*) causes and contributes risk for oral clefting disorders. We hypothesized that genes regulated by IRF6 are also involved in oral clefting disorders. We used five criteria to identify potential IRF6 target genes; differential gene expression in skin taken from wild type and *Irf6*-deficient murine embryos, localization to the Van der Woude syndrome 2 (*VWS2*) locus at 1p36–1p32, overlapping expression with *Irf6*, presence of a conserved predicted binding site in the promoter region, and a mutant murine phenotype that was similar to the *Irf6* mutant mouse. Previously, we observed altered expression for 573 genes; 13 were located in the murine region syntenic to the *VWS2* locus. Two of these genes, *Wdr65* and *Stratifin*, met four of five criteria. *Wdr65* was a novel gene that encoded a predicted protein of 1250 amino acids with two WD domains. As potential targets for Irf6 regulation, we hypothesized that disease-causing mutations will be found in *WDR65* and *Stratifin* in individuals with VWS or VWS-like syndromes. We identified a potentially etiologic missense mutation in *WDR65* in a person with VWS who does not have an exonic mutation in

Correspondence to: Brian C. Schutte, 5162 Biomedical and Physical Science Building, Microbiology and Molecular Genetics, Michigan State University, East Lansing, MI 48823, TEL: 517-884-5346, FAX: 517- 353-8957, schutteb@msu.edu.

URLs
BLAST: http://www.ncbi.nlm.nih.gov/
Boxshade: http://www.ch.embnet.org/software/BOX_form.html
dbSNP: http://www.ncbi.nlm.nih.gov/projects/SNP/
Ensembl genome browser: http://www.ensembl.org
Matinspector: http://www.genomatix.de
Primer3: http://frodo.wi.mit.edu/cgi-bin/primer3/primer3_www.cgi
Tcoffee: http://igs-server.cnrs-mrs.fr/Tcoffee/tcoffee_cgi/index.cgi
UCSC Genome Browser: http://genome.ucsc.edu
VISTA browser: http://pipeline.lbl.gov

IRF6. The expression and mutation data were consistent with the hypothesis that *WDR65* was a novel gene involved in oral clefting.

Keywords

cleft lip and palate; mutation; gene expression; syndrome; genomic; microvilli; WD domain; transcription factor

INTRODUCTION

Interferon regulatory factor 6 (IRF6) is a member of the Interferon regulatory factor family of transcription factors. IRF6 shares the highly-conserved helix-turn-helix penta-tryptophan DNA binding domain and the interferon associated protein interaction domain, suggesting it functions as a transcription factor [Kondo et al., 2002]. Mutations in the *IRF6* gene are responsible for two autosomal dominant syndromic forms of cleft lip with or without cleft palate, Van der Woude and popliteal pterygium syndromes [Kondo et al., 2002]. Additionally, a study performed on 11 geographically distinct populations showed an association between the V274I polymorphism in IRF6 and isolated cleft lip and palate [Zucchero et al., 2004], and subsequent work identified a SNP in the binding site for the TFAP2A transcription factor that altered binding [Rahimov et al., 2008]. This body of work demonstrates that *IRF6* is an integral component for development of the lip and palate. Other genes and loci have been shown to play a role in human clefting using candidate gene [Jugessur et al., 2009] and genome wide strategies [Birnbaum et al., 2009]. We hypothesize that by studying potential regulatory targets of IRF6 we will identify new genes involved in development of the lip and palate. In this study, we used a genomic approach to find genes that might be regulated by IRF6. Based on our observations, we hypothesize that *WDR65* and *Stratifin* (*SFN* or *14-3-3 sigma*) are necessary for human craniofacial development, and mutations in these genes may be found in families affected with VWS and VWS-related disorders.

MATERIALS and METHODS

Identification of genes in the murine syntenic region of the *VWS2* locus

The *VWS2* locus was mapped between *D1S2697* and *D1S230* [Koillinen et al., 2001]. We used the UCSC genome browser (build hg18) to determine the probable region of synteny in the murine genome, and used the Ensembl genome browser to obtain gene content and sequence. We used Matinspector to identify potential IRF binding sites in the 1kb region upstream of the transcription start site of the VWS2 candidate genes. To enrich for functional IRF binding sites, only putative sites conserved in rat, mouse, and human were used (VISTA Browser).

SYBR Green Real-time PCR

Microarray expression data (GDS2359) [Ingraham et al., 2006] was verified with SYBR Green real-time PCR analysis using primer pairs designed with PrimerExpress (Applied Biosystems, Foster City, CA) and amplified using Power SYBR Green PCR Master Mix (Applied Biosystems) with 1ng of cDNA derived from 17.5 dpc wild type and *Irf6* mutant murine skin RNA [Ingraham et al., 2006]. Standard curves were performed as recommended, and a *Rpl4* primer set was used as the internal control. Sequence for all primers used in this study are listed in Supplemental Table I.

Structure and expression of mouse *Wdr65* and its human ortholog

Wdr65 was PCR amplified from a testis cDNA library (BD Biosciences) using the forward primer MF2TOPO and the reverse primer MR23 and cloned into pENTR/D-TOPO cloning vector (Invitrogen, Carlsbad, CA). 5' RACE was performed as recommended (Ambion, Foster City, CA). These products were sequenced on both the forward and the reverse strands at the University of Iowa DNA Core Facility. The human ortholog of *Wdr65* was found utilizing tBLASTn and tBLASTx programs. Only one protein was highly similar over the entire sequence. The human and murine protein sequences were aligned using Tcoffee and Boxshade. Exons of murine *Wdr65* were aligned with human genomic sequence to determine the exon boundaries of *WDR65* using Sequencher 4.2 (GeneCodes, Ann Arbor, MI).

In-situ hybridization was performed on coronal sections of murine embryonic heads. The processing of the sections and probes were performed as previously described [Goudy et al., 2010]. The probes for *Wdr65* were made from the Riken clone 1110020C03 (MGC Image#1478343) that contained 630 bases of exons 20–23. For the antisense probe, the plasmid was linearized with *Sac*I and labeled with T3 polymerase. For the sense probe, the plasmid was linearized with SalI, and labeled with T7 polymerase. For semi-quantitative PCR experiments, cDNA was obtained from the following sources; multi-tissue panels (BD Bioscience), human (Stratagene) and murine skin (Origene, Rockville, MD), C57Bl/6 embryonic stem cells, and from murine palate obtained by Laser Capture Microdissection (Pixel II system, Molecular Devices, Sunnyvale, CA). For microdissection, embryos at different developmental stages were embedded in OTC and frozen in liquid nitrogen. Tissue sections (7 μm) were dehydrated using serial ethanol concentrations, followed by xylene. The desired cells were captured, and RNA was extracted using a TRIzol solution, followed by RNeasy and DNase I cleanup, and cDNA was made as recommended (Ambion).

DNA sequence analysis of samples from patients

We obtained written informed consent from all subjects and approval for all protocols from the Institutional Review Boards at the University of Iowa, the University of São Paulo State and CONEP/Brazil, and the Karolinska Institutet. Subjects were examined by a clinical geneticist or by a genetic counselor, and diagnoses were made as described previously for VWS [Kondo et al., 2002], VWS2 [Koillinen et al., 2001] and BPS [Shanske et al., 2004]. Sample collection and processing and DNA sequence analysis were performed as previously described [Kondo et al., 2002].

RESULTS

Altered expression of genes in *VWS2* locus in *Irf6* mutant skin

Previous linkage studies of VWS pedigrees suggest little evidence for genetic heterogeneity for VWS. However, one VWS-like pedigree from Finland was found not to be linked to the *IRF6* region. Rather, linkage was observed at the interval 1p36–1p32, and the authors named this locus *VWS2* [Koillinen et al., 2001]. As one criterion for a regulatory target for IRF6, we hypothesized that the *VWS2* locus contains such a gene. The *VWS2* locus was mapped between the markers *D1S2697* and *D1S230* [Koillinen et al., 2001], near the genes *CLCNKB* and *INADL*, respectively. The murine orthologs of these two genes were located at 140,676,436 and at 97,887,844 on murine chromosome 4. In this region, the 694 genes and their order were conserved, confirming a syntenic relationship (Fig. 1a).

As a second criterion for genes regulated by Irf6, we hypothesized that their expression would be altered in tissues that lack *Irf6*. We took advantage of our previous microarray experiments that identified 573 differentially expressed genes between wild type and *Irf6*-

deficient murine embryos at 17.5 days post conception (dpc) [Ingraham et al., 2006]. Of these genes, 13 were located in the syntenic region of the *VWS2* locus (Table I). The microarray data (Fig. 1b) were verified by real-time PCR for *Irf6*, *Wdr65* and *Sfn* (Fig. 1c). Two of the 13 genes were omitted because the probes mapped to an intron of one gene (*Hdac1*) or because the amount of mRNA in normal skin was deemed insignificant in a second gene (*Sh2d5*). Thus, we limited further studies to the remaining 11 candidate genes.

Comparison of *Irf6* expression with target candidates

We hypothesized that target genes of Irf6 will show spatial and temporal expression patterns similar to *Irf6*. *Irf6* showed tissue-specific expression, and of the eleven candidate genes, only *Wdr65* had a distinct tissue-specific pattern (Fig. 2). We also compared temporal expression patterns in whole murine embryos. *Irf6* expression was first seen in embryonic stem cells, disappeared, reappeared at 7 dpc embryos and peaks in 17 dpc embryos [Kondo et al., 2002]. Only two candidate genes, *Wdr65* and *Paqr7*, showed similar changes in temporal expression during embryonic development (Fig 2). As a final comparison, we measured gene expression during development of the palate. For this analysis, cDNA was generated from whole palates before fusion (12.5–13.5 dpc), at fusion (14.5 dpc), after fusion (15.5 dpc), and from the medial edge epithelium (MEE). As expected from previous studies [Ingraham et al., 2006; Richardson et al., 2006], *Irf6* was present in these tissues, except in the MEE isolated from *Irf6*-deficient embryos (Fig. 2). Most candidate genes showed constitutive expression in all palatal tissues, even in the absence of *Irf6*. Significantly, *Wdr65* was present in the 14.5 dpc MEE, but was absent in MEE from *Irf6*-deficient embryos. In sum, these expression studies were most consistent with the hypothesis that *Wdr65* is a target for regulation by Irf6.

IRF binding sites near candidate genes

IRF6 contains the highly conserved DNA binding domain of the IRF family, and a previous study showed that this domain binds to the consensus IRF binding site [Little et al., 2009]. In an effort to determine which of the eleven candidate genes could be direct targets of Irf6, we searched for putative IRF binding sites near each gene. A single conserved putative binding site was found for *Wdr65* and *Sfn* (Table I). However, the binding site identified for *Wdr65* was found in an exon of *Ebna1bp2*, a gene found 63 bp upstream of *Wdr65* and transcribed in the opposite direction.

Murine phenotypes of candidate genes

As a final criterion for potential Irf6 target genes, we compared the phenotypes of mutant murine strains to determine if the function of the candidate genes were consistent with craniofacial development. Of the eleven candidate genes, seven have been mutated in mice (Table 1). Of these, only *Sfn* mutant mice showed cleft palate and other craniofacial abnormalities [Herron et al., 2005].

Genomic and cDNA Structure of *WDR65*

Overall, *Sfn* and *Wdr65* met four of the five criteria as candidates for regulation by IRF6 (Fig. 3). We then wished to screen these two genes for DNA variants that may cause VWS and VWS-like syndromes. However, *WDR65* was a novel gene whose complete structure needed to be determined. When viewed in the ENSEMBL genomic database, we observed a predicted gene, ENSMUST00000081921 upstream from the Riken clone 1110020C03. We hypothesized that the predicted gene represented the 5' end of the Riken clone. Using a PCR primer designed from each of these clones, MF2TOPO and MR23 (Fig. 4a), we amplified a 4 kb product from a murine testis cDNA library. Using 5' RACE we amplified a 238 bp

product. When sequenced, these products generated a complete cDNA whose length was 3958 bp. When aligned with the murine genomic sequence, *Wdr65* has 23 exons.

To determine the human ortholog, we performed a BLAST search with *Wdr65* and identified human cDNA clones, including NM_152489. This clone contained the first eleven exons, with 5' and 3' untranslated regions (UTRs) and a polyA tail (Fig. 4b). PCR experiments using human and murine cDNA, resulted in the identification of a shorter transcript, with only eleven exons, that we named *WDR65b* and *Wdr65b*, respectively. To clone the large human *WDR65* transcript, we performed PCR experiments using primers designed to the most 5' and 3' human cDNA clones. We amplified a 4126 bp product that contains 24 exons from human testis cDNA. This larger human transcript is similar to the murine *Wdr65* transcript, except it has an additional exon, exon 19, which adds 33 amino acids. In total, *WDR65* human and murine genes produced two transcripts, *WDR65b* (11 exons), and a larger transcript, *WDR65*, with 24 exons in human and 23 exons in mouse. The long transcript was the major expressed isoform in both human and mouse (Supplemental Fig. 1). The human and murine *WDR65* genes were predicted to encode proteins that are highly similar (Supplemental Fig. 2). And in each species, both the long and short isoforms were predicted to encode two WD-repeat functional domains (Supplemental Fig. 3). WD-repeat domains comprise a highly conserved motif defined by starting with GH (Gly-His) followed by 23–41 amino acid core and ending with WD (Trp-Asp).

Expression of *Wdr65* in craniofacial tissues

To identify cell types that expressed *Wdr65* in craniofacial structures, *in situ* experiments were performed on coronal sections from 14.5, and 15.5 dpc murine embryos. At 14.5 dpc the palates were juxtaposed and strong *Wdr65* staining was seen in the nasal epithelium and detected in the medial edge epithelium (MEE) (Fig. 5a). In 15.5 dpc mice the expression was very strong in the nasal respiratory epithelium and epidermis, but was not seen in the oral epithelium (Fig. 5b). The expression of *Wdr65* in the nasal epithelium was limited to the respiratory epithelium and not the olfactory epithelium. Significantly, we observed that the strong oral and nasal respiratory epithelia expression seen in the wild type (Fig. 5c) was markedly decreased or absent in the *Irf6* mutant sections (Fig. 5d). These data are consistent with the hypothesis that *Wdr65* is a candidate target of Irf6 and is strongly, though not completely, dependent on Irf6 for proper expression.

Sequencing two *VWS2* candidates, *SFN* and *WDR65* in three patient populations

In the *VWS2*-linked pedigree, we sequenced the entire *SFN* gene and all exons for *WDR65*. *SFN* has a single exon, and the putative binding site for IRF6 was located in a multi-species conserved region located 900 bp upstream of the transcriptional start site. The only DNA variant observed in these two regions was rs3065004, a highly polymorphic microsatellite repeat located in the 3'UTR of *SFN*. For *WDR65*, we observed that the sequence was heterozygous for two DNA variants, rs663824 (non-synonymous, Asn241Asp) and rs603123 (synonymous). These DNA variants were not etiologic because they were observed in samples from unaffected individuals.

For this study, we sequenced samples from 48 individuals with VWS that lacked a mutation in any exon for the 5'UTR and coding region of *IRF6* [Kondo et al., 2002; de Lima et al., 2009]. To test whether mutations in *SFN* and *WDR65* contributed to VWS, we sequenced *SFN* as above, but limited our analysis of *WDR65* to the exons coding for the WD repeat domain (exons 7 through 10). These exons were chosen because a deleterious mutation would most likely be located in a functional domain [Braun et al., 2006]. We found a missense mutation in exon 10 (c.1567G>T; p.Asp523Tyr) in one individual from Brazil with

VWS (Fig. 6a). This residue is conserved through chicken (Fig. 6b). Since this mutation was not seen in controls and significantly changes the biochemical properties of a conserved residue, we conclude that it is potentially etiologic. To screen for other DNA variants, we performed DNA sequence analysis on all 24 exons in 32 DNA samples. We observed 21 additional DNA variants. Genotypes for all DNA variants were not significantly different from Hardy-Weinberg equilibrium, and all but one were detected previously in control populations (Supplemental Table II), suggesting that they are not etiologic. The one novel DNA variant was located in intron 5 and its function was unknown.

Bartsocas-Papas syndrome (BPS) is also referred to as lethal popliteal pterygium syndrome because the affected population has overlapping characteristics of PPS. But unlike PPS, BPS is autosomal recessive, and has a more severe phenotype that leads to early lethality. DNA from a patient with BPS was obtained [Shanske et al., 2004] and the whole gene for *SFN* and all the exons for *WDR65* were sequenced. We observed no DNA variants in *SFN*. In *WDR65,* we observed eight rare DNA variants, seven were in introns and one was synonymous (Supplemental Table II). Two of these DNA variants were not found in other populations, but they were found in introns and their function was unknown. Overall, we cannot exclude *WDR65* as the causative gene for this recessive disorder since no heterozygous DNA variants were observed in the patient who is from a consanguineous family.

DISCUSSION

The goal of this study was to identify new candidate genes for cleft lip and palate that are regulated by *IRF6*. *IRF6*, a gene critical for palatal development, encodes a putative transcription factor, and we hypothesized that gene targets would be potential cleft genes. From our genomic approach we identified two strong candidate targets for Irf6, *Sfn*, and the novel gene *Wdr65*. While mutation analyses at two syndromic clefting populations, VWS2 and BPS, failed to support a direct role for *SFN* and *WDR65*, a potentially etiologic missense mutation in *WDR65* was discovered in a patient with VWS. Therefore, DNA variation in *WDR65* may contribute to human oral clefting.

We identified and cloned *WDR65,* a gene that produced two transcripts of 11 and 24 exons. Both transcripts encoded two WD domains. Proteins containing WD-repeat domains are found most commonly in eukaryotic organisms. This is an extremely large family of proteins comprising over 100 human proteins with various functions [Smith et al., 1999]. Most WD-repeat proteins have 4–16 WD-repeats, and a minimum of four repeats were needed to form a proper tertiary structure, and seven produced the most stable structure [Li and Roberts, 2001]. Since WDR65 only has two predicted WD-repeats, it may not function in the traditional fashion of WD-repeat domain proteins.

The missense mutation found in a patient with VWS suggests that *WDR65* plays a role in the fusion of lip and palate. The strongest expression of *Wdr65* was seen in simple epithelium, specifically the ventral nasal respiratory epithelium, but not the nasal olfactory epithelium. Three other genes have a similar pattern of expression and have a role in palatal development, *Gabrb3* [Hagiwara et al., 2003], *Hoxa-2* [Nazarali et al., 2000] and *Tbx1* [Goudy et al., 2010]. These genes all showed strong nasal epithelial expression during palatal fusion. The expression in the nasal epithelia suggests a role for this epithelium during the fusion of the palate to the nasal septum, which occurs at the same time as palatal fusion.

The increase in *Wdr65* expression in whole palates and in 14.5 dpc MEE correlated with the development and dissolution of the epithelial seam. Previous studies suggest involvement in at least two potential pathways. First, several WD-repeat domain proteins function in

programmed cell death, which could facilitate the dissolution of the medial edge seam in the MEE [Li and Roberts, 2001]. Second, *WDR65* was identified recently as a candidate for a gene involved in cilial function [McClintock et al., 2008]. This hypothesis was based on the observation that expression of 1110020C03RIK was statistically overrepresented in tissues that contain highly ciliated cells, including olfactory epithelium, testis, vomeronasal organ, trachea and lung. However, immuno-staining shows direct staining of microvilli in bronchial epithelium, fallopian tube and epididymis mucosa (www.proteinatlas.org). It is interesting to speculate about a role for WDR65 in microvilli. During the adhesion and fusion of the primary palate, microvilli appeared, then disappeared and finally reappeared on the epithelial surfaces [Millicovsky and Johnston, 1981]. Further studies are needed to address the potential roles of *Irf6* and *WDR65* in apoptosis and changes in microvilli appearance during the development of the lip and palate.

Supplementary Material

Refer to Web version on PubMed Central for supplementary material.

Acknowledgments

The authors wish to acknowledge technical assistance from M. Malik, L. Henkle, K. Boyer, and R. Williamson. We would also like to thank Kevin Knudtson at the University of Iowa DNA Core Facility. This work was supported in part by the Predoctoral Training Program in Genetics 5 T32 GM08629 (N.K.R.), US National Institutes of Health grant DE16215 (J.C.M., B.C.S.), DE08559 (J.C.M.) and DE13513 (B.C.S., N.K.R.).

REFERENCES

Bell SM, Schreiner CM, Schultheis PJ, Miller ML, Evans RL, Vorhees CV, Shull GE, Scott WJ. Targeted disruption of the murine Nhe1 locus induces ataxia, growth retardation, and seizures. Am J Physiol. 1999; 276:C788–C795. [PubMed: 10199808]

Birnbaum S, Ludwig KU, Reutter H, Herms S, Steffens M, Rubini M, Baluardo C, Ferrian M, Almeida de Assis N, Alblas MA, Barth S, Freudenberg J, Lauster C, Schmidt G, Scheer M, Braumann B, Berge SJ, Reich RH, Schiefke F, Hemprich A, Potzsch S, Steegers-Theunissen RP, Potzsch B, Moebus S, Horsthemke B, Kramer FJ, Wienker TF, Mossey PA, Propping P, Cichon S, Hoffmann P, Knapp M, Nothen MM, Mangold E. Key susceptibility locus for nonsyndromic cleft lip with or without cleft palate on chromosome 8q24. Nat Genet. 2009; 41:473–477. [PubMed: 19270707]

Braun TA, Shankar SP, Davis S, O'Leary B, Scheetz TE, Clark AF, Sheffield VC, Casavant TL, Stone EM. Prioritizing regions of candidate genes for efficient mutation screening. Hum Mutat. 2006; 27:195–200. [PubMed: 16395665]

de Lima RL, Hoper SA, Ghassibe M, Cooper ME, Rorick NK, Kondo S, Katz L, Marazita ML, Compton J, Bale S, Hehr U, Dixon MJ, Daack-Hirsch S, Boute O, Bayet B, Revencu N, Verellen-Dumoulin C, Vikkula M, Richieri-Costa A, Moretti-Ferreira D, Murray JC, Schutte BC. Prevalence and nonrandom distribution of exonic mutations in interferon regulatory factor 6 in 307 families with Van der Woude syndrome and 37 families with popliteal pterygium syndrome. Genet Med. 2009; 11:241–247. [PubMed: 19282774]

Goudy S, Law A, Sanchez G, Baldwin HS, Brown C. Tbx1 is necessary for palatal elongation and elevation. Mech Dev. 2010; 127:292–300. [PubMed: 20214979]

Hagiwara N, Katarova Z, Siracusa LD, Brilliant MH. Nonneuronal expression of the GABA(A) beta3 subunit gene is required for normal palate development in mice. Dev Biol. 2003; 254:93–101. [PubMed: 12606284]

Herron BJ, Liddell RA, Parker A, Grant S, Kinne J, Fisher JK, Siracusa LD. A mutation in stratifin is responsible for the repeated epilation (Er) phenotype in mice. Nat Genet. 2005; 37:1210–1212. [PubMed: 16200063]

Ingraham CR, Kinoshita A, Kondo S, Yang B, Sajan S, Trout KJ, Malik MI, Dunnwald M, Goudy SL, Lovett M, Murray JC, Schutte BC. Abnormal skin, limb and craniofacial morphogenesis in mice

deficient for interferon regulatory factor 6 (Irf6). Nat Genet. 2006; 38:1335–1340. [PubMed: 17041601]

Jugessur A, Farlie PG, Kilpatrick N. The genetics of isolated orofacial clefts: from genotypes to subphenotypes. Oral Dis. 2009; 15:437–453. [PubMed: 19583827]

Koillinen H, Wong FK, Rautio J, Ollikainen V, Karsten A, Larson O, Teh BT, Huggare J, Lahermo P, Larsson C, Kere J. Mapping of the second locus for the Van der Woude syndrome to chromosome 1p34. Eur J Hum Genet. 2001; 9:747–752. [PubMed: 11781685]

Kondo S, Schutte BC, Richardson RJ, Bjork BC, Knight AS, Watanabe Y, Howard E, Ferreira De Lima RL, Daack-Hirsch S, Sander A, McDonald-McGinn DM, Zackai EH, Lammer EJ, Aylsworth AS, Ardinger HH, Lidral AC, Pober BR, Moreno L, Arcos-Burgos M, Valencia C, Houdayer C, Bahuau M, Moretti-Ferreira D, Richieri-Costa A, Dixon MJ, Murray JC. Mutations in IRF6 cause Van der Woude and popliteal pterygium syndromes. Nat Genet. 2002; 32:285–289. [PubMed: 12219090]

Li D, Roberts R. WD-repeat proteins: structure characteristics, biological function, and their involvement in human diseases. Cell Mol Life Sci. 2001; 58:2085–2097. [PubMed: 11814058]

Little HJ, Rorick NK, Su LI, Baldock C, Malhotra S, Jowitt T, Gakhar L, Subramanian R, Schutte BC, Dixon MJ, Shore P. Missense mutations that cause Van der Woude syndrome and popliteal pterygium syndrome affect the DNA-binding and transcriptional activation functions of IRF6. Hum Mol Genet. 2009; 18:535–545. [PubMed: 19036739]

McClintock TS, Glasser CE, Bose SC, Bergman DA. Tissue expression patterns identify mouse cilia genes. Physiol Genomics. 2008; 32:198–206. [PubMed: 17971504]

Millicovsky G, Johnston MC. Active role of embryonic facial epithelium: new evidence of cellular events in morphogenesis. J Embryol Exp Morphol. 1981; 63:53–66. [PubMed: 7310294]

Nazarali A, Puthucode R, Leung V, Wolf L, Hao Z, Yeung J. Temporal and spatial expression of Hoxa-2 during murine palatogenesis. Cell Mol Neurobiol. 2000; 20:269–290. [PubMed: 10789828]

Rahimov F, Marazita ML, Visel A, Cooper ME, Hitchler MJ, Rubini M, Domann FE, Govil M, Christensen K, Bille C, Melbye M, Jugessur A, Lie RT, Wilcox AJ, Fitzpatrick DR, Green ED, Mossey PA, Little J, Steegers-Theunissen RP, Pennacchio LA, Schutte BC, Murray JC. Disruption of an AP-2alpha binding site in an IRF6 enhancer is associated with cleft lip. Nat Genet. 2008; 40:1341–1347. [PubMed: 18836445]

Richardson RJ, Dixon J, Malhotra S, Hardman MJ, Knowles L, Boot-Handford RP, Shore P, Whitmarsh A, Dixon MJ. Irf6 is a key determinant of the keratinocyte proliferation-differentiation switch. Nat Genet. 2006; 38:1329–1334. [PubMed: 17041603]

Shanske AL, Hoper SA, Krahn K, Schutte BC. Mutations in IRF6 do not cause Bartsocas-Papas syndrome in a family with two affected sibs. Am J Med Genet A. 2004; 128A:431–433. [PubMed: 15264293]

Smith TF, Gaitatzes C, Saxena K, Neer EJ. The WD repeat: a common architecture for diverse functions. Trends Biochem Sci. 1999; 24:181–185. [PubMed: 10322433]

Zucchero TM, Cooper ME, Maher BS, Daack-Hirsch S, Nepomuceno B, Ribeiro L, Caprau D, Christensen K, Suzuki Y, Machida J, Natsume N, Yoshiura K, Vieira AR, Orioli IM, Castilla EE, Moreno L, Arcos-Burgos M, Lidral AC, Field LL, Liu YE, Ray A, Goldstein TH, Schultz RE, Shi M, Johnson MK, Kondo S, Schutte BC, Marazita ML, Murray JC. Interferon regulatory factor 6 (IRF6) gene variants and the risk of isolated cleft lip or palate. N Engl J Med. 2004; 351:769–780. [PubMed: 15317890]

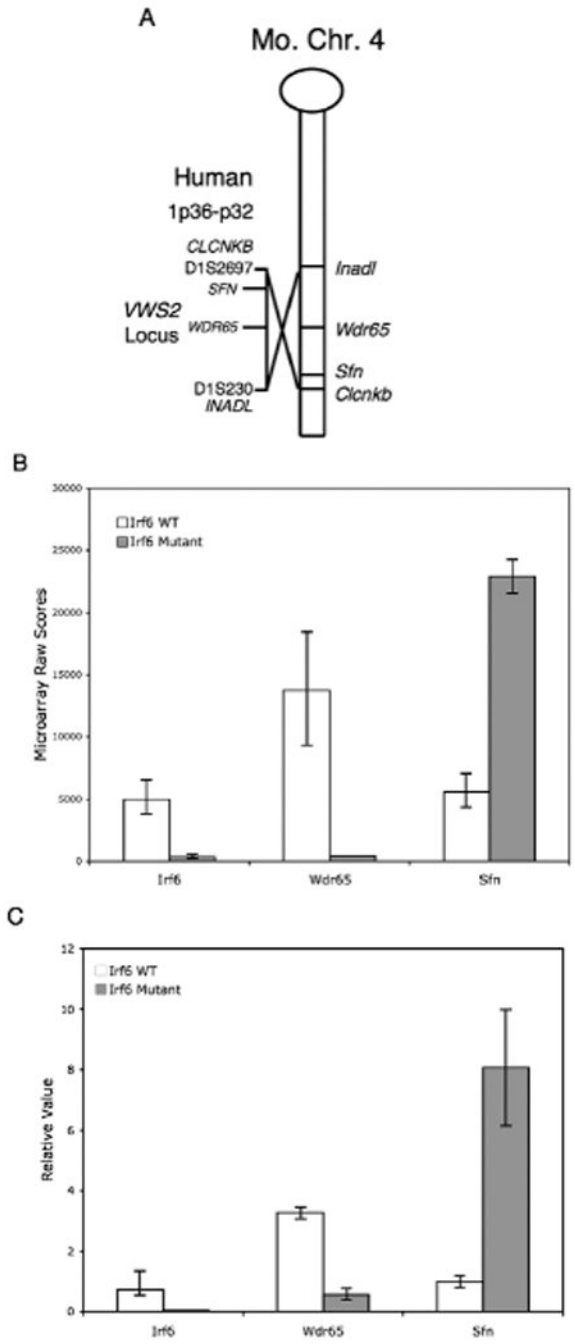

Figure 1.

(A) *VWS2* locus and the syntenic region in mouse. The *VWS2* locus is located on human chromosome 1p36-p31. The murine syntenic region is inverted on murine chromosome 4 and contained *Wdr65* and *Sfn*. Relative expression of *Irf6*, *Wdr65*, and *Sfn* in skin isolated from 17.5 dpc wild type and *Irf6*-deficient murine embryos by (B) microarray analysis, (C) real-time PCR.

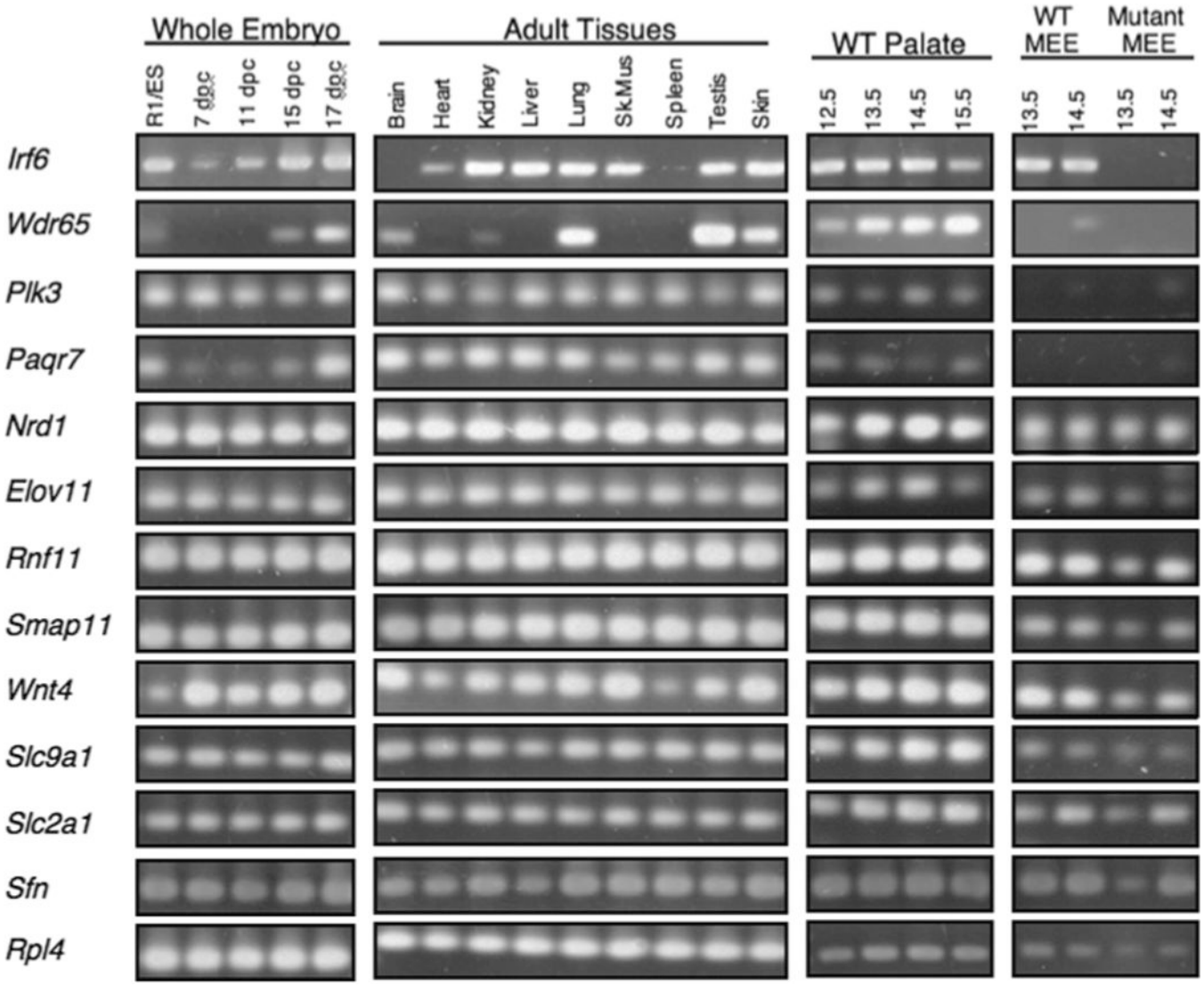

Figure 2.
Expression of *VWS2* candidate genes compared with *Irf6*. PCR products are shown for the gene listed at left and the cDNA source listed at the top.

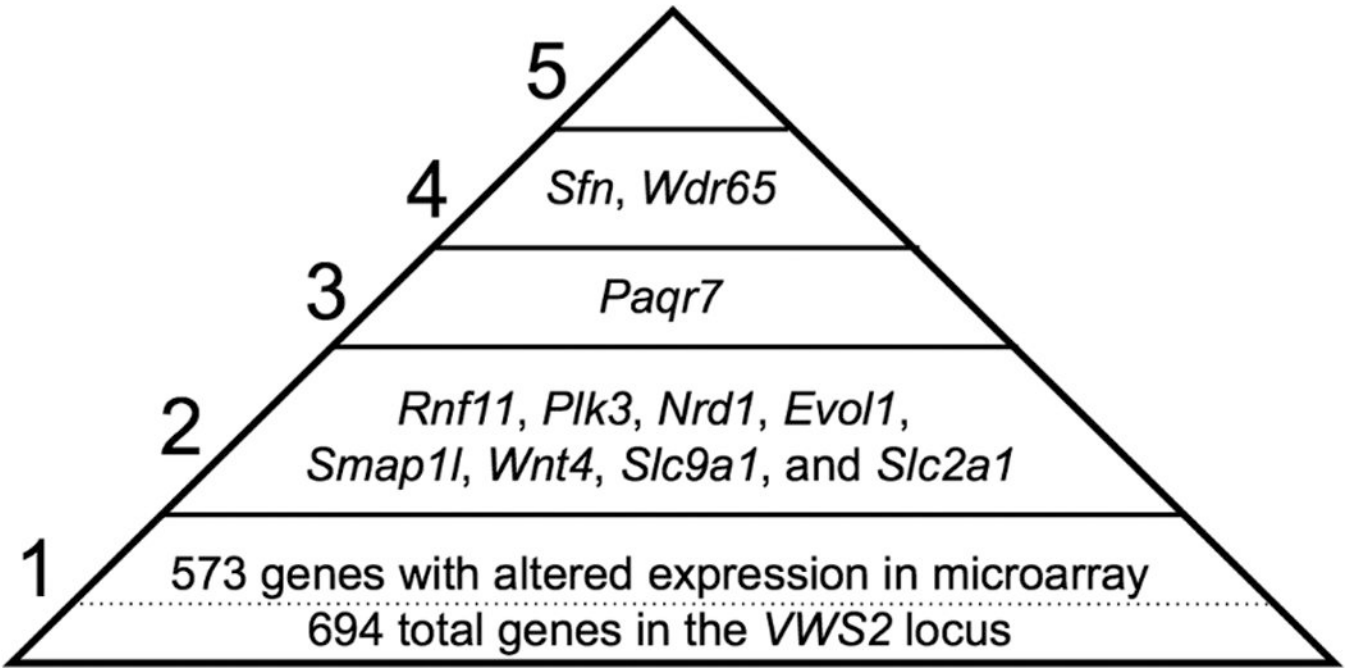

Figure 3.
Probability pyramid for Irf6 gene targets. The numbers of criteria met by the indicated genes are listed at left.

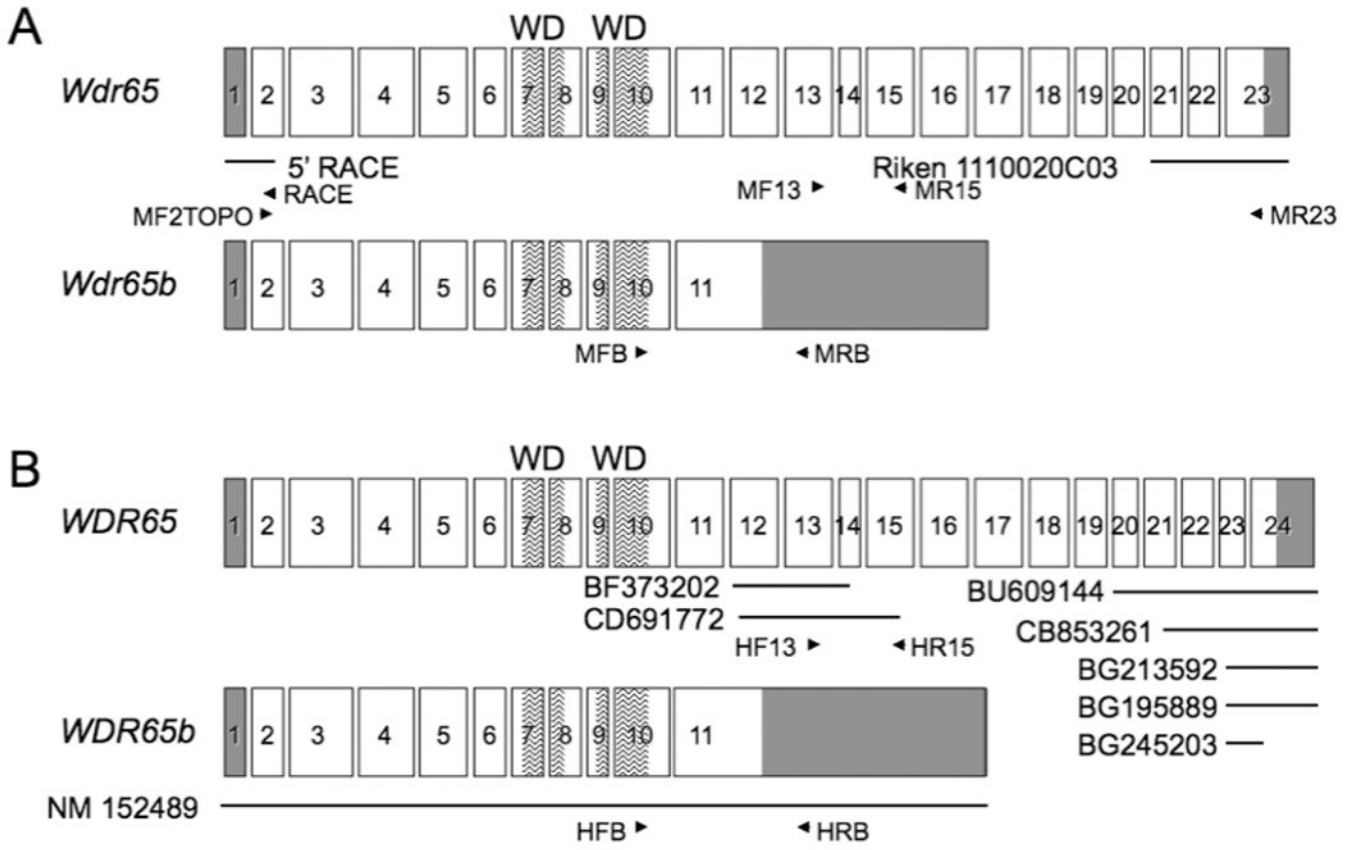

Figure 4.

Genomic and cDNA structure of *WDR65* gene. *Wdr65* in mouse (A) and its human orotholog (B) are shown with the untranslated region (shaded), open reading frame (open), and WD repeat domains (lines). The sequenced 5' RACE product is shown by the line below exons 1 and 2. Primer locations are indicated by the arrowheads. The human clone NM152489 and the ESTs support the *WDR65* and *WDR65b* structures, while the Riken clone 1110020C03 supports the 3' end of *Wdr65*.

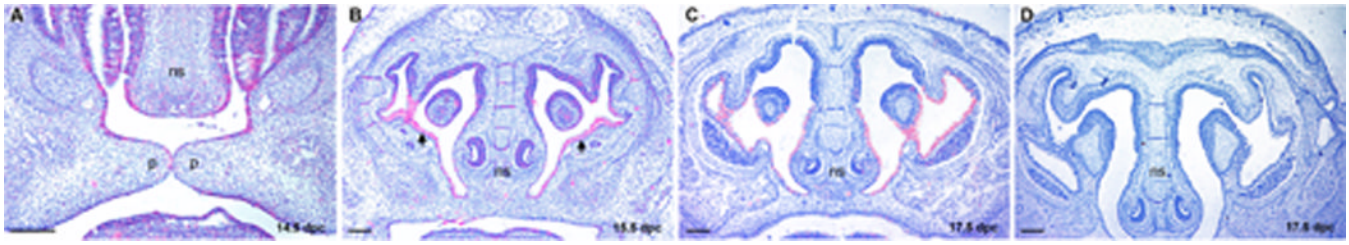

Figure 5.

Expression of *Wdr65* in oral and nasal tissues. (A) *In situ* hybridization at 14.5 dpc showed staining in the medial edge and nasal epithelium of murine palatal shelves (p) and epithelium of nasal septum (ns). (B) Strong staining was seen in the nasal epithelium (black arrowheads) of 15.5 dpc mice and also in the cutaneous epidermis. (C) Strong staining was observed in nasal epithelium of wild type mice at 17.5 dpc. (D) Staining was lost in 17.5 dpc embryos that lack *Irf6*.

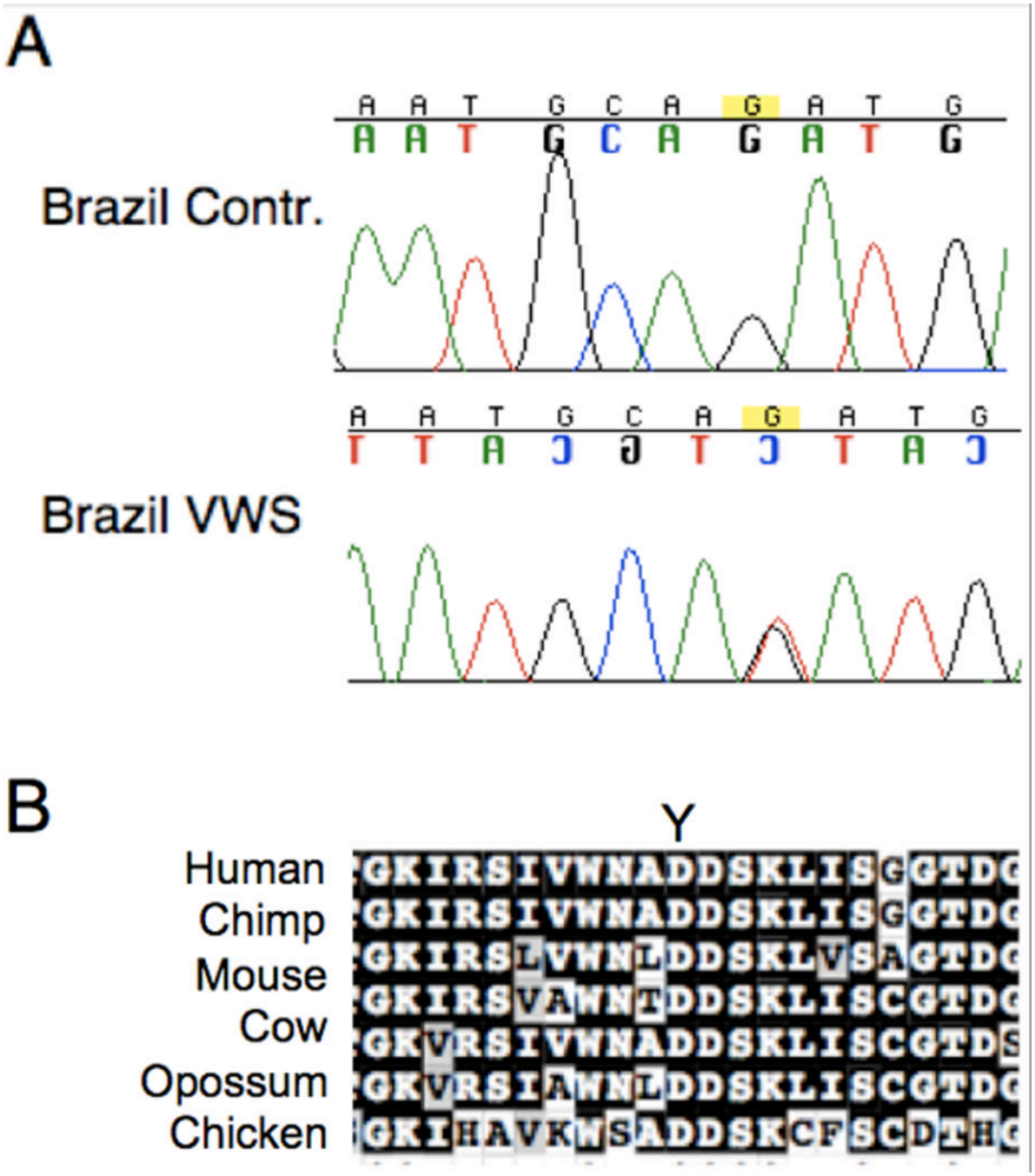

Figure 6.
Missense mutation in *WDR65* in a patient with VWS. (A) Chromatograms of a Brazilian control and a Brazilian patient with VWS displaying a G to T base pair change which results in a p.Asp523Tyr missense mutation. (B) The Tyrosine (Y) missense mutation is shown above the conserved Aspartic acid residue (D).

TABLE I

VWS2 Candidate Genes.

Gene	Hu Chr	Fold[a]	WT Mean	Mut Mean	ISRE[b]	Dysm[c]	Cranio Dysm[c]	Cleft[c]
WDR65	1p34.2	−15	1304	83	0.69	N/A	N/A	N/A
PLK3	1p34.1	−13	298	23	0	No	No	no
PAQR7	1p36.1	−4	346	91	0	N/A	N/A	N/A
NRD1	1p32.3	−3	1080	320	0	No	No	No
ELOVL1	1p34.2	−3	3588	1265	0	N/A	N/A	N/A
RNF11	1p32.3	−2	1681	719	0	N/A	N/A	N/A
SMAP2	1p34.2	−2	479	222	0	No	No	No
WNT4	1p36.1	2	454	1058	0	Yes	No	No
SLC9A1	1p36.1	3	322	824	0	Yes	No	No
SLC2A1	1p34.2	4	1413	4009	0	Yes	No	No
SFN	1p36.1	3	691	2372	0.96	Yes	Yes	Yes

Listed are the gene name, chromosome location in human genome (Hu Chr), fold change in microarray for 17.5 dpc skin (GDS2359), mean value from microarray for 17.5 dpc skin from wild type (WT) and mutant (Mut) embryos, matrix score for predicted IRF Stimulatory Response Element (ISRE) identified by MatInspector that is also conserved in human, mouse, and rat, and located within 1kb of the transcription start site, observed dysmorphology (Dysm), cranial dysmorphology (Cranio Dysm) and oral cleft (Cleft) in knockout mouse.

[a] A decrease in expression between wild type to mutant is indicated by a negative value.

[b] No ISRE identified that meets criteria (0).

[c] No available phenotype data (N/A), dysmorphology is present (yes) or absent (no).